Synthesis of CdS nano-spheres by a simple and fast sonochemical method at room temperature

Paula A.L. Lopes [a], Maurício Brandão Santos [a], Artur José Santos Mascarenhas [a,b], Luciana Almeida Silva [a,b,*]

[a] Instituto de Química, Universidade Federal da Bahia, Campus de Ondina, Salvador 40170-290, Bahia, Brazil
[b] Instituto Nacional de Ciência e Tecnologia, INCT, de Energia e Ambiente, Universidade Federal da Bahia, 40170-290 Salvador-BA, Brazil

ABSTRACT

Nano-spheres of hexagonal CdS were prepared by a sonochemical method using $CdCl_2$ and $Na_2S_2O_3$ as precursors, with different molar ratios of cadmium and sulfur in starting solutions, in ethylene glycol and cetyltrimethylammonium bromide (CTAB) as a surfactant. The XRD patterns for all samples presented the set of peaks characteristic of CdS in hexagonal phase. The crystallite size decreases as the sulfur content increased in the starting solution as a consequence of the quick release of sulfide ions trapped in the micelles formed by the CTAB surfactant, which controls the CdS nanoparticles growth. The diffuse reflectance spectroscopy (DRS) results have shown that it is possible to tune the emission of visible light of the CdS semiconductor changing only the starting Cd:S ratios in this synthesis procedure.

© 2014 Elsevier B.V. All rights reserved.

1. Introduction

CdS is an n-type semiconductor with band gap energy of 2.4 eV. Among the II–VI semiconductors, CdS is of special interest because it has great potential applications in photocatalysis and optoelectronic devices because of its high photosensitivity coupled with the ability to tune the emission in the visible light range with different crystal structures, sizes and shapes [1–3]. Cadmium sulfide (CdS) has the thermodynamic potential to drive water splitting into hydrogen and oxygen with visible light illumination. According to Matsumura et al. [1], higher hydrogen production rates and higher photoefficiencies are obtained with bulk-phase hexagonal CdS when compared to bulk-phase cubic CdS suspensions. In this way, it is important to develop synthesis methods that are capable to obtain CdS in pure hexagonal phase with sizes and shapes suitable for photocatalytic proposals. There are different methods used to synthesize CdS, such as solvothermal synthesis [4], hydrothermal process [5], microwave irradiation [6], sonochemistry process [7,8], sonochemistry-assisted microwave [9]. In general, cubic-phase CdS (c-CdS) has been obtained by the method that uses low temperatures and, in these cases, it is possible to obtain quantum-sized particles. In contrast, hexagonal-phase CdS (hex-CdS) in a "wurtzite" crystal structure is generally obtained at high temperature, which results in large particles. However, sonochemistry methods usually yield CdS in hexagonal phase, probably due to the high temperatures and pressures produced in imploding cavitation bubbles.

Sonochemistry uses high power ultrasonic waves (20 kHz - 10 MHz) to promote chemical reactions [10,11] and has been successfully applied in the synthesis of new materials, since they provide smaller particle size and higher surface area than reported by other methods. The advantages of sonochemical methods are high velocity rates, controllable reaction conditions, capacity to form uniform shapes, narrow distributions of particle size and high purity [12]. Ghows et al. [13] applied a sonochemical method to prepare hexagonal and/or cubic CdS and concluded that the crystal structure is governed by the kind of cadmium salt solution used in the preparation of the sample, besides the ultrasonic waves intensity and kind of solvent. Recently, we developed a sonochemical method to synthesize nanostructures of bismuth sulfide in 1D and 3D, in which the shape and quality of the nanocrystals depend on the type of solvent used in the synthesis procedure [14]. In the present work, we used a sonochemichal method to prepare h-CdS using $CdCl_2$ and $Na_2S_2O_3$ as the precursors for preparing nanoparticles of CdS in unique hexagonal phase with high morphological homogeneity. Besides, we evaluated the influence of different Cd:S ratios in the quality and size of the nanoparticles and the possibility of tuning the emission of visible light with the different synthesis conditions.

2. Experimental

Nano-sized CdS was prepared using appropriated amounts of the precursors $CdCl_2$ and $Na_2S_2O_3$ dissolved in ethylene glycol

* Corresponding author at: Instituto de Química, Universidade Federal da Bahia, Campus de Ondina, Salvador 40170-20, Bahia, Brazil.
E-mail address: las@ufba.br (L.A. Silva).

and cetyltrimethylammonium bromide (CTAB) as a surfactant. The molar ratios of cadmium and sulfur in starting solutions were 1:2, 1:4, 1:6, and 1:8 and the samples were so named S2, S4, S6, and S8, respectively. The starting solutions were exposed to high-intensity ultrasound irradiation using an ultrasonic waves source R2D091109, Unique, under ambient air for 15 min with power adjusted at 80 W. When each reaction was finished, yellow precipitates were obtained. After being cooled to room temperature, the precipitates were centrifuged, washed with distilled water, absolute ethanol, and acetone in sequence, and dried in air at room temperature. The powders were characterized by X-ray diffraction (Shimadzu XRD6000), using CuK_α, Ni-filtered radiation, and scanning rate of $2° 2\theta min^{-1}$, in a 2θ range of 5–80°, at 35 kV and 15 mA. The average crystallite sizes were calculated from the X-ray line broadening at $2\theta=43.78°$ using the Debye–Scherrer equation. Diffuse reflectance spectra were recorded on a spectrometer Thermo Scientific Evolution 600 UV–vis by using a praying mantis accessory. SEM images were taken in JSM-6610LV scanning electron microscopy (JEOL) operated at 20 kV after gold metalization. The BET areas were taken from the treatment of N_2 adsorption isotherms determined at 77 K, after vacuum pretreating the samples at 323 K for 12 h in a Micromeritics ASAP2020 automated sorptometer.

3. Results and discussion

Fig. 1 shows XRD patterns of the materials obtained from different Cd:S ratios. The XRD patterns for all samples present three broad peaks in 24.8°, 26.5° and 28.1° (2θ). This set of peaks is characteristic of CdS in hexagonal phase. Meanwhile, in all cases such peaks are not well resolved, but one can see more well-defined peaks in XRD patterns of the samples with low Cd:S ratios, especially in the sample S2. The broad peaks in the XRD patterns,
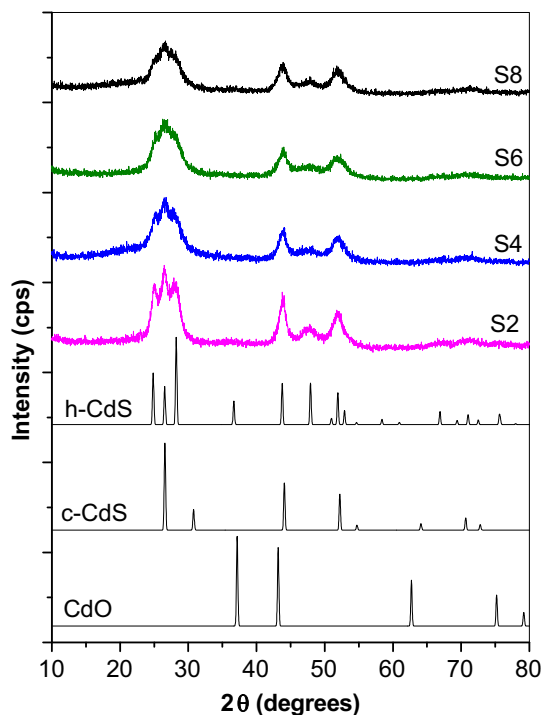
especially for Samples S4–S8, can be a consequence of the small particle sizes and also due to an effect of crystallinity. In any of the cases, we observe segregated phase.

The crystallite size of the samples can be estimated with the Debye–Scherrer's equation from XRD data:

$$D = \frac{0.89\lambda}{B \cos \theta} \tag{1}$$

where λ is the X-ray wavelength of 1.541 Å, θ is the Bragg diffraction angle and B is the full width at half maximum (FWHM) of 2θ [15,16]. B values were taken with Gaussian fitting of the data scattering graphic from 41° to 46° (2θ). Crystallite sizes calculated using the Bragg diffraction angle at $2\theta=43.78°$ (the best resolved peak) are shown in Table 1. For all samples, we can observe a clear tendency in decrease of crystallite size as increase the sulfur concentration in the starting solution, suggesting that it is possible to control the particles dimensions with the amount of sulfur available in the reaction medium.

The sonochemical mechanism of CdS formation takes into consideration the radical species obtained from the solvent ethylene glycol and also the acidity of solution in the end of the process:

$$C_2H_6O_2 \;))))) \; C_2H_5O_2^\bullet + H^\bullet \tag{2}$$

$$S_2O_3^{2-} + 2H^\bullet \rightarrow S^{2-} + 2H^+ + SO_3^{2-} \tag{3}$$

$$S^{2-} + CTA^+ \rightarrow (CTA^+)_nS^{2-} \; (\text{micelles}) \tag{4}$$

$$(CTA^+)_nS^{2-} + Cd^{2+} \rightarrow CdS \tag{5}$$

The CdS nanoparticles growth should be controlled by CTAB micelles loaded with sulfide ions [17]. For high content of sulfur in the starting solution, sulfite ions are released from the CTAB micelles more quickly, limiting the particle growth. Meanwhile, in the cases where the sulfur content is low, the formed particles are larger, probably due to the slow release of sulfide ions, which allows growing of the particles with higher crystal quality.

The treatment of isotherm data using BET and BJH methods resulted in the textural properties in Table 1. Samples S2 to S6 presented low surface areas, as expected for type III (Figure S1)

Table 1
Crystallite diameter, textural properties and band bag energy of the samples S2–S8.

Sample	Crystallite diameter (nm)	S_{BET} ($m^2 g^{-1}$)	D_{pore} (nm)	Eg (eV)
S2	8.4	17.4	29.1	2.41
S4	7.6	15.5	38.9	2.51
S6	5.3	16.7	31.0	2.58
S8	5.2	44.6	6.63	2.72

Fig. 1. XRD patterns of the powders obtained from different ratios of Cd:S in the starting solution and ICSD patterns for the phases CdS wurtzite (pdf # 01–075–1545–41–1049); cubic CdS (pdf # 01–089–0440 10–454) and CdO (pdf # 01–073–2245–5–640).
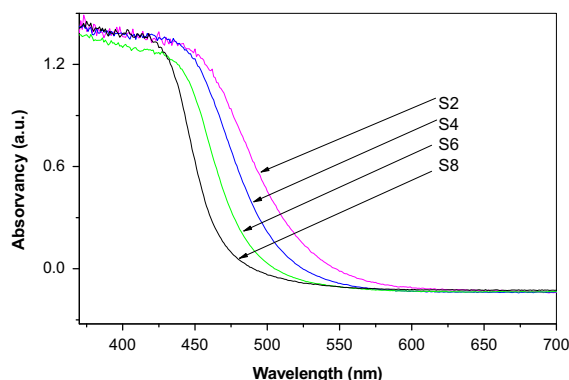

Fig. 2. Diffuse reflectance spectra (DRS) of of the powders obtained from different ratios of Cd:S in the starting solution.
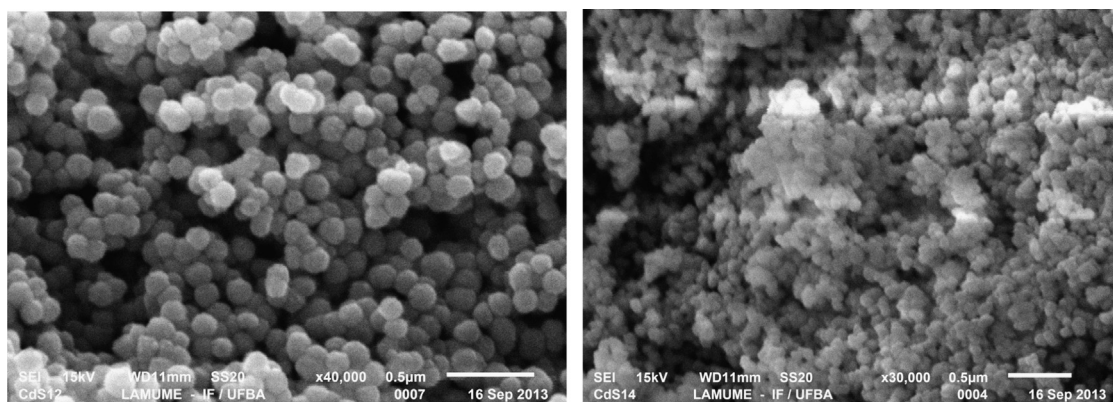
Fig. 3. SEM micrographs of the samples S2 and S4.

isotherm materials, and the average pore diameter is the transition range between meso and macropores. On the one hand, sample S8 present a type IV isotherm (Fig. S1), typical of mesoporous materials and has the highest value for BET surface area among all samples ($45\ \mathrm{m^2\,g^{-1}}$), with pore diameter of approximately 7 nm.

The SEM micrographs of the materials with the best resolved XRD patterns (samples S2 and S4) are shown in Fig. 2. SEM images reveal that CdS was obtained as small spheres with high morphological homogeneity when the Cd:S ration in the stating solution was 1:2 (S2 sample) and the morphological homogeneity decreases when the ratio is 1:4 (S4 sample) as well as spheres diameter. The diameters of the spheres (around 100 nm) are in contrast with the crystallites diameters (8 nm) obtained from the Debye–Scherrer's equation, suggesting that the spheres are formed of agglomerated of smaller crystallites similar to Bi_2S_3 in which the nano-spheres are actually superstructures formed by nanorods with diameter of 11–15 nm [14].

The diffuse reflectance spectra of the samples are depicted in Fig. 3. As seen, as the amount of sulfur in starting solution increases a blue shift is observed as a consequence of the decrease in particle size (Table 1). To obtain the optical band gap energies, the geometrical method was applied to the experimental data, assuming direct band transitions [18], which uses the relation below:

$$I = A(hn - E_g)^{1/2} \tag{6}$$

where I is the absorption intensity, A is a coefficient, and $h\nu$ is the photon energy. The values of E_g were obtained by extrapolation of the best linear fit between I^2 and $h\nu$ up to the point where it crosses the ordinate axis. The band gap values for the samples are also described in Table 1.

The dimension of all semiconductor particles obtained here are below a critical radius of approximately 10 nm, when the charge carriers appear to behave quantum mechanically as a simple particle in a box [19], which suggests that these materials could act as quantum-sized semiconductors. The increase of band gap energy with the decrease of particle size is an evidence that is possible to tune the emission of visible light of the CdS semiconductor changing only the starting Cd:S ratios in this synthesis procedure.

4. Conclusions

The sonochemical method showed to be fast, simple and efficient for preparing of nano-sized CdS in hexagonal phase as small spheres with high morphological homogeneity. Our results revealed that is possible to control the growth of the nanoparticles only varying the sulfur content in the starting solution and consequently to tune the emission of visible-light of the CdS.

Appendix A. Supporting information

Supplementary data associated with this article can be found in the online version at http://dx.doi.org/10.1016/j.matlet.2014.07.173.

References

[1] Matsumura M, Furukawa S, Saho Y, Tsubomura HJ. Phys Chem 1985;89: 1327–9.
[2] Silva LA, Ryu SY, Choi J, Choi W, Hoffmann MRJ. Phys Chem C 2008;112: 12069–73.
[3] Melo MO, Silva LAJ. Photochem Photobio A: Chem 2011;226:36–41.
[4] Zhao JG, Hua ZH, Yao Y. Superlattice Microst 2013;61:146–51.
[5] Cao Y, Hua P, Jia D. Appl Surf Sci 2013;265:771–7.
[6] Ebadi M, Abedini S, Rezai O, Rad MMJ. Ind Eng Chem, 2014. http://dx.doi.org/10.1016/j.jiec.2013.12.085.
[7] Behboudnia M, Khanbabaee B. Colloid Surface A 2006;290:229–32.
[8] Li HL, Zhu YC, Chen SG, Palchik O, Xiong JP, Koltypin Y, et al. Sol Stat Chem 2003;172:102–10.
[9] Tai G, Guo W. Ultrason Sonochem 2008;15:350–6.
[10] Suslick KS, Hyeon TW, Fang MW. Chem Mater 1996;8:2172–9.
[11] Suslick KS, Choe SB, Cichowlas AA, Grinstaff MW. Nature 1991;353:414–6.
[12] Gedanken A. Ultrason Sonochem 2004;11:47–55.
[13] Ghows N, Entezari MH. Ultrason Sonochem 2011;18:269–75.
[14] Mesquita PRR, Almeida JS, Teixeira LSG, Ferreira da Silva A, Silva LAJ. Braz Chem Soc 2013;24:280–4.
[15] Almeida CG, Andrade HMC, Mascarenhas AJS, Silva LA. Mater Lett 2010;64: 1088–90.
[16] Guimarães TBF, Pepe I, Ferreira da Silva A, Mangrich AS, de Andrade JB, Silva LA. J Alloys Compd 2009;481:654–8.
[17] Emin S, Sogoshi N, Nakabayashi S, Villeneuve M, Dushkin CJ. Photochem Photobio A: Chem 2009;207:173–80.
[18] Nisar J, Silva LA, Almeida CG, Mascarenhas AJS, Wang B, Araujo CM, et al. Phys Status Solidi C 2012;9:1593–6.
[19] Hoffmann RM, Martin SC, Choi W, Bahnemann DW. Chem Rev 1995;95:69–96.